

Scattering, Form Factors, and Exotics from Lattice QCD

Colin Morningstar

Carnegie Mellon University

KLF Collaboration Meeting
JLab, Newport News, VA

February 12, 2020



Outline

- excited-states in lattice QCD
- finite-volume energies \Rightarrow scattering phase shifts
- multi-hadron correlators and stochastic LapH method
- hadron resonance properties: masses, decay widths
- time-like pion form factor
- scalar glueball
- tetraquark operators and the $K_0^*(700)$, $a_0(980)$
- string breaking
- current efforts: baryon-baryon scattering
- some recent lattice QCD highlights
- key points:
 - calculations at physical point now happening
 - can deal with disconnected diagrams

Excited states from correlation matrices

- energies from temporal correlations $C_{ij}(t) = \langle 0 | \bar{O}_i(t) O_j(0) | 0 \rangle$
- in finite volume, energies are discrete (neglect wrap-around)

$$C_{ij}(t) = \sum_n Z_i^{(n)} Z_j^{(n)*} e^{-E_n t}, \quad Z_j^{(n)} = \langle 0 | O_j | n \rangle$$

- not practical to do fits using above form
- define new correlation matrix $\tilde{C}(t)$ using a single rotation

$$\tilde{C}(t) = U^\dagger C(\tau_0)^{-1/2} C(t) C(\tau_0)^{-1/2} U$$

- columns of U are eigenvectors of $C(\tau_0)^{-1/2} C(\tau_D) C(\tau_0)^{-1/2}$
- choose τ_0 and τ_D large enough so $\tilde{C}(t)$ diagonal for $t > \tau_D$
- effective energies

$$\tilde{m}_\alpha^{\text{eff}}(t) = \frac{1}{\Delta t} \ln \left(\frac{\tilde{C}_{\alpha\alpha}(t)}{\tilde{C}_{\alpha\alpha}(t + \Delta t)} \right)$$

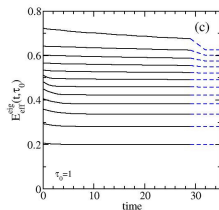
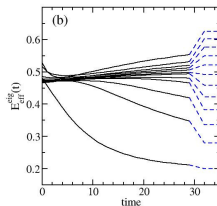
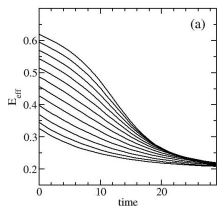
tend to N lowest-lying stationary state energies in a channel

- 2-exponential fits to $\tilde{C}_{\alpha\alpha}(t)$ yield energies E_α and overlaps $Z_j^{(n)}$

Correlator matrix toy model

- Example: 12×12 correlator matrix with $N_e = 200$ eigenstates

$$E_0 = 0.20, \quad E_n = E_{n-1} + \frac{0.08}{\sqrt{n}}, \quad Z_j^{(n)} = \frac{(-1)^{j+n}}{1 + 0.05(j-n)^2}.$$



- left: effective energies of diagonal elements of correlator matrix
- middle: effective energies of eigenvalues of $C(t)$
- right: effective energies of eigenvalues of $C(\tau_0)^{-1/2} C(t) C(\tau_0)^{-1/2}$ for $\tau_0 = 1$

Building blocks for single-hadron operators

- important to use **good** operators to see signal before noise growth
- building blocks: covariantly-displaced LapH-smearred quark fields
- stout links $\tilde{U}_j(x)$
- Laplacian-Heaviside (LapH) smeared quark fields

$$\tilde{\psi}_{a\alpha}(x) = \mathcal{S}_{ab}(x, y) \psi_{b\alpha}(y), \quad \mathcal{S} = \Theta \left(\sigma_s^2 + \tilde{\Delta} \right)$$

- 3d gauge-covariant Laplacian $\tilde{\Delta}$ in terms of \tilde{U}
- displaced quark fields:

$$q_{a\alpha j}^A = D^{(j)} \tilde{\psi}_{a\alpha}^{(A)}, \quad \bar{q}_{a\alpha j}^A = \tilde{\psi}_{a\alpha}^{(A)} \gamma_4 D^{(j)\dagger}$$

- displacement $D^{(j)}$ is product of smeared links:

$$D^{(j)}(x, x') = \tilde{U}_{j_1}(x) \tilde{U}_{j_2}(x+d_2) \tilde{U}_{j_3}(x+d_3) \dots \tilde{U}_{j_p}(x+d_p) \delta_{x', x+d_{p+1}}$$

- to good approximation, LapH smearing operator is

$$\mathcal{S} = V_s V_s^\dagger$$

- columns of matrix V_s are eigenvectors of $\tilde{\Delta}$

Extended operators for single hadrons

- quark displacements build up orbital, radial structure

Meson configurations



Baryon configurations



$$\bar{\Phi}_{\alpha\beta}^{AB}(\mathbf{p}, t) = \sum_{\mathbf{x}} e^{i\mathbf{p}\cdot(\mathbf{x} + \frac{1}{2}(\mathbf{d}_\alpha + \mathbf{d}_\beta))} \delta_{ab} \bar{q}_{b\beta}^B(\mathbf{x}, t) q_{a\alpha}^A(\mathbf{x}, t)$$

$$\bar{\Phi}_{\alpha\beta\gamma}^{ABC}(\mathbf{p}, t) = \sum_{\mathbf{x}} e^{i\mathbf{p}\cdot\mathbf{x}} \varepsilon_{abc} \bar{q}_{c\gamma}^C(\mathbf{x}, t) \bar{q}_{b\beta}^B(\mathbf{x}, t) \bar{q}_{a\alpha}^A(\mathbf{x}, t)$$

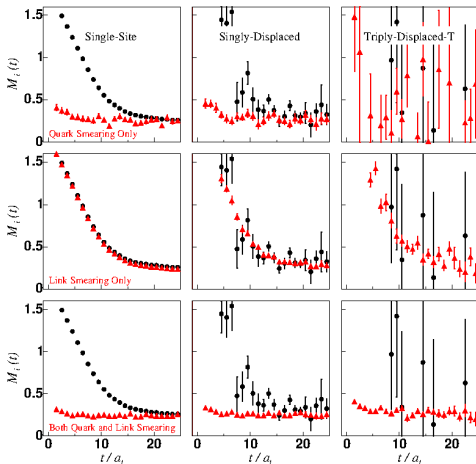
- group-theory projections onto irreps of lattice symmetry group

$$\bar{M}_l(t) = c_{\alpha\beta}^{(l)*} \bar{\Phi}_{\alpha\beta}^{AB}(t) \quad \bar{B}_l(t) = c_{\alpha\beta\gamma}^{(l)*} \bar{\Phi}_{\alpha\beta\gamma}^{ABC}(t)$$

- definite momentum \mathbf{p} , irreps of little group of \mathbf{p}

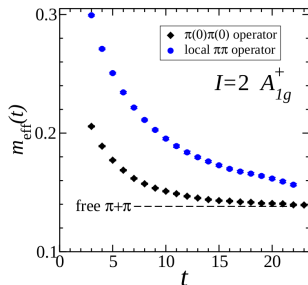
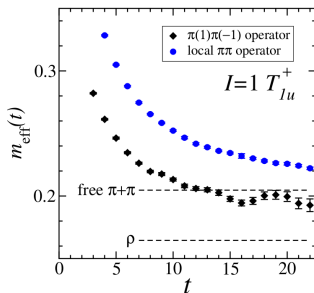
Importance of smeared fields

- effective masses of 3 selected nucleon operators shown
- noise reduction of displaced-operators from link smearing
 $n_\rho = 2.5, n_\rho = 16$
- quark-field smearing
 $\sigma_s = 4.0, n_\sigma = 32$ reduces excited-state contamination



Two-hadron operators

- comparison of $\pi(\mathbf{k})\pi(-\mathbf{k})$ and localized $\sum_{\mathbf{x}} \pi(\mathbf{x})\pi(\mathbf{x})$ operators



- important to use superposition of products of single-hadron operators of definite momenta
- efficient construction, generalizes to three or more hadrons

Quark propagation

- quark propagator Q is inverse D^{-1} of Dirac matrix
 - rows/columns involve lattice site, spin, color
 - very large $N_{\text{tot}} \times N_{\text{tot}}$ matrix for each flavor
- for $64^3 \times 128$ lattice, $N_{\text{tot}} \sim 400$ million
- not feasible to compute (or store) all elements of D^{-1}
- point-to-all trick for **local** operators: use translation invariance

$$\sum_{\mathbf{y}} \sum_{\mathbf{x}} Q^{(a)}(\mathbf{y}, t_f | \mathbf{x}, t_i) Q^{(b)}(\mathbf{y}, t_f | \mathbf{x}, t_i) \dots \longrightarrow \sum_{\mathbf{y}} Q^{(a)}(\mathbf{y}, t_f | \mathbf{x}_0, t_i) Q^{(b)}(\mathbf{y}, t_f | \mathbf{x}_0, t_i) \dots$$

- cannot use this trick for **good** multi-hadron operators

$$\sum_{\mathbf{y}_1, \mathbf{y}_2, \dots} \sum_{\mathbf{x}_1, \mathbf{x}_2, \dots} Q^{(a)}(\mathbf{y}_1, t_f | \mathbf{x}_1, t_i) Q^{(b)}(\mathbf{y}_2, t_f | \mathbf{x}_2, t_i) \dots$$

- our solution: the stochastic LapH method!
- other methods

Stochastic estimation of quark propagators

- do not need exact inverse of Dirac matrix $D[U]$
- introduce Z_4 noise vectors η in the LapH subspace

$$\eta_{\alpha k}(t), \quad t = \text{time}, \quad \alpha = \text{spin}, \quad k = \text{eigenvector number}$$

- solve $D[U]X^{(r)} = \eta^{(r)}$ for each of N_R noise vectors $\eta^{(r)}$, then obtain a Monte Carlo estimate of all elements of D^{-1}

$$D_{ij}^{-1} \approx \frac{1}{N_R} \sum_{r=1}^{N_R} X_i^{(r)} \eta_j^{(r)*}$$

- variance reduction using noise dilution
- dilution introduces projectors $P^{(a)}$, then define

$$\eta^{[a]} = P^{(a)}\eta, \quad X^{[a]} = D^{-1}\eta^{[a]}$$

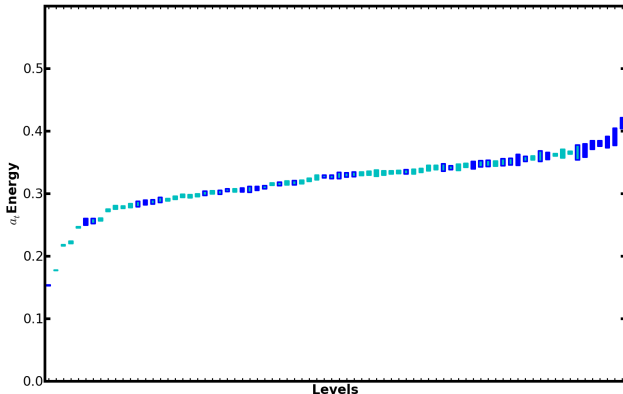
to obtain Monte Carlo estimate with drastically reduced variance

$$D_{ij}^{-1} \approx \frac{1}{N_R} \sum_{r=1}^{N_R} \sum_a X_i^{(r)[a]} \eta_j^{(r)[a]*}$$

Bosonic $I = \frac{1}{2}$, $S = 1$, T_{1u} channel

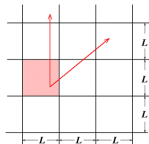
- finite-volume stationary-state energies: “staircase” plot
- $32^3 \times 256$ lattice for $m_\pi \sim 240$ MeV
- use of single- and two-meson operators only
- blue: levels of max overlaps with SH optimized operators

kaon T_{1u} 32



Quantum numbers in toroidal box

- periodic boundary conditions in cubic box
 - not all directions equivalent \Rightarrow using J^{PC} is wrong!!



- label stationary states of QCD in a periodic box using irreps of cubic space group **even in continuum limit**

- zero momentum states: little group O_h

$$A_{1a}, A_{2ga}, E_a, T_{1a}, T_{2a}, \quad G_{1a}, G_{2a}, H_a, \quad a = g, u$$

- on-axis momenta: little group C_{4v}

$$A_1, A_2, B_1, B_2, E, \quad G_1, G_2$$

- planar-diagonal momenta: little group C_{2v}

$$A_1, A_2, B_1, B_2, \quad G_1, G_2$$

- cubic-diagonal momenta: little group C_{3v}

$$A_1, A_2, E, \quad F_1, F_2, G$$

- include G parity in some meson sectors (superscript $+$ or $-$)

Spin content of cubic box irreps

- numbers of occurrences of Λ irreps in J subduced

J	A_1	A_2	E	T_1	T_2
0	1	0	0	0	0
1	0	0	0	1	0
2	0	0	1	0	1
3	0	1	0	1	1
4	1	0	1	1	1
5	0	0	1	2	1
6	1	1	1	1	2
7	0	1	1	2	2

J	G_1	G_2	H	J	G_1	G_2	H
$\frac{1}{2}$	1	0	0	$\frac{9}{2}$	1	0	2
$\frac{3}{2}$	0	0	1	$\frac{11}{2}$	1	1	2
$\frac{5}{2}$	0	1	1	$\frac{13}{2}$	1	2	2
$\frac{7}{2}$	1	1	1	$\frac{15}{2}$	1	1	3

Scattering phase shifts in lattice QCD timeline

- **Lüscher 1984**: energies of multi-hadron stationary states in finite volume can yield scattering phase shifts
- **Rummukainen and Gottlieb 1995**: nonzero total momenta
- **Kim, Sachrajda, and Sharpe 2005**: revisited
- explosion of papers since then
- **Briceno 2014**: generalized to arbitrary spin, multiple channels

Two-particle correlator in finite-volume

- correlator of two-particle operator σ in finite volume

$$C^L(P) = \begin{array}{c} \sigma \text{---} \text{---} \sigma^\dagger + \sigma \text{---} iK \text{---} \sigma^\dagger \\ + \sigma \text{---} iK \text{---} iK \text{---} \sigma^\dagger + \dots \end{array}$$

- Bethe-Salpeter kernel

$$iK = \begin{array}{c} \text{---} \text{---} \\ \text{---} \text{---} \end{array} + \begin{array}{c} \text{---} \text{---} \\ \text{---} \text{---} \end{array} + \begin{array}{c} \text{---} \text{---} \\ \text{---} \text{---} \end{array} + \begin{array}{c} \text{---} \text{---} \\ \text{---} \text{---} \end{array} + \begin{array}{c} \text{---} \text{---} \\ \text{---} \text{---} \end{array}$$

- $C^\infty(P)$ has branch cuts where two-particle thresholds begin
- momentum quantization in finite volume: cuts \rightarrow series of poles
- C^L poles: two-particle energy spectrum of finite volume theory

Corrections from finite momentum sums

- finite-volume momentum sum is infinite-volume integral plus correction \mathcal{F}

The diagram shows an equality between three terms. On the left, a dashed box encloses two vertices: a black circle on top and a blue circle on bottom, connected by two arcs (one black, one blue). This is equal to the sum of two terms. The first term is the same two-vertex structure without the dashed box. The second term is a vertical dashed line with a horizontal line crossing it, labeled \mathcal{F} .

- define the following quantities: A , A' , invariant scattering amplitude $i\mathcal{M}$

The diagram shows three equations defining quantities in terms of diagrams:

- $A = \sigma + \sigma \circlearrowleft iK + \sigma \circlearrowleft iK \circlearrowleft iK + \dots$
- $A' = \sigma^\dagger + iK \circlearrowleft \sigma^\dagger + iK \circlearrowleft iK \circlearrowleft \sigma^\dagger + \dots$
- $i\mathcal{M} = iK + iK \circlearrowleft iK + iK \circlearrowleft iK \circlearrowleft iK + \dots$

In these diagrams, σ and σ^\dagger are circles with a horizontal line through them. iK is a circle with a horizontal line through it. The arcs between circles are black or blue, and some circles have a black dot on top.

Quantization condition

- subtracted correlator $C_{\text{sub}}(P) = C^L(P) - C^\infty(P)$ given by

$$C_{\text{sub}}(P) = \begin{array}{c} \textcircled{A} \text{---} \mathcal{F} \text{---} \textcircled{A'} \\ + \textcircled{A} \text{---} \mathcal{F} \text{---} \textcircled{iM} \text{---} \mathcal{F} \text{---} \textcircled{A'} \\ + \textcircled{A} \text{---} \mathcal{F} \text{---} \textcircled{iM} \text{---} \mathcal{F} \text{---} \textcircled{iM} \text{---} \mathcal{F} \text{---} \textcircled{A'} \\ + \dots \end{array}$$

- sum geometric series

$$C_{\text{sub}}(P) = A \mathcal{F} (1 - iM\mathcal{F})^{-1} A'.$$

- poles of $C_{\text{sub}}(P)$ are poles of $C^L(P)$ from $\det(1 - iM\mathcal{F}) = 0$
- key tool: for $g_c(\mathbf{p})$ spatially contained and regular

$$\frac{1}{L^3} \sum_{\mathbf{p}} g_c(\mathbf{p}) = \int \frac{d^3k}{(2\pi)^3} g_c(\mathbf{k}) + O(e^{-mL})$$

$$\frac{1}{L^3} \sum_{\mathbf{p}} \frac{g_c(\mathbf{p}^2)}{(\mathbf{p}^2 - a^2)} = \frac{1}{L^3} \sum_{\mathbf{p}} \frac{g_c(a^2)}{(\mathbf{p}^2 - a^2)} + \int \frac{d^3k}{(2\pi)^3} \frac{g_c(\mathbf{p}^2) - g(a^2)}{(\mathbf{p}^2 - a^2)} + O(e^{-mL})$$

- work in spatial L^3 volume with periodic b.c.
- total momentum $\mathbf{P} = (2\pi/L)\mathbf{d}$, where \mathbf{d} vector of integers
- calculate lab-frame energy E of two-particle interacting state in lattice QCD
- boost to center-of-mass frame by defining:

$$E_{\text{cm}} = \sqrt{E^2 - \mathbf{P}^2}, \quad \gamma = \frac{E}{E_{\text{cm}}},$$

- assume N_d channels
- particle masses m_{1a}, m_{2a} and spins s_{1a}, s_{2a} of particle 1 and 2
- for each channel, can calculate

$$\mathbf{q}_{\text{cm},a}^2 = \frac{1}{4}E_{\text{cm}}^2 - \frac{1}{2}(m_{1a}^2 + m_{2a}^2) + \frac{(m_{1a}^2 - m_{2a}^2)^2}{4E_{\text{cm}}^2},$$
$$u_a^2 = \frac{L^2 \mathbf{q}_{\text{cm},a}^2}{(2\pi)^2}, \quad \mathbf{s}_a = \left(1 + \frac{(m_{1a}^2 - m_{2a}^2)}{E_{\text{cm}}^2} \right) \mathbf{d}$$

Quantization condition re-expressed

- E related to S matrix (and phase shifts) by

$$\det[1 + F^{(P)}(S - 1)] = 0$$

- F matrix in $JLSa$ basis states given by

$$\begin{aligned} \langle J' m_{J'} L' S' a' | F^{(P)} | J m_J L S a \rangle = & \delta_{a'a} \delta_{S'S} \frac{1}{2} \left\{ \delta_{J'J} \delta_{m_{J'} m_J} \delta_{L'L} \right. \\ & \left. + \langle J' m_{J'} | L' m_{L'} S m_S \rangle \langle L m_L S m_S | J m_J \rangle W_{L' m_{L'}; L m_L}^{(Pa)} \right\} \end{aligned}$$

- total ang mom J, J' , orbital L, L' , spin S, S' , channels a, a'
- W given by

$$\begin{aligned} -i W_{L' m_{L'}; L m_L}^{(Pa)} = & \sum_{l=|L'-L|}^{L'+L} \sum_{m=-l}^l \frac{Z_{lm}(\mathbf{s}_a, \gamma, u_a^2)}{\pi^{3/2} \gamma u_a^{l+1}} \sqrt{\frac{(2L'+1)(2l+1)}{(2L+1)}} \\ & \times \langle L' 0, l 0 | L 0 \rangle \langle L' m_{L'}, l m | L m_L \rangle. \end{aligned}$$

- above expressions apply for both distinguishable and indistinguishable particles

RGL shifted zeta functions

- compute Rummukainen-Gottlieb-Lüscher (RGL) shifted zeta functions \mathcal{Z}_{lm} using

$$\begin{aligned}\mathcal{Z}_{lm}(\mathbf{s}, \gamma, u^2) &= \sum_{\mathbf{n} \in \mathbb{Z}^3} \frac{\mathcal{Y}_{lm}(\mathbf{z})}{(z^2 - u^2)} e^{-\Lambda(z^2 - u^2)} + \delta_{l0} \frac{\gamma\pi}{\sqrt{\Lambda}} F_0(\Lambda u^2) \\ &+ \frac{i^l \gamma}{\Lambda^{l+1/2}} \int_0^1 dt \left(\frac{\pi}{t}\right)^{l+3/2} e^{\Lambda t u^2} \sum_{\substack{\mathbf{n} \in \mathbb{Z}^3 \\ \mathbf{n} \neq 0}} e^{\pi i \mathbf{n} \cdot \mathbf{s}} \mathcal{Y}_{lm}(\mathbf{w}) e^{-\pi^2 \mathbf{w}^2 / (t\Lambda)}\end{aligned}$$

- where

$$\mathbf{z} = \mathbf{n} - \gamma^{-1} \left[\frac{1}{2} + (\gamma - 1) \mathbf{s}^{-2} \mathbf{n} \cdot \mathbf{s} \right] \mathbf{s},$$

$$\mathbf{w} = \mathbf{n} - (1 - \gamma) \mathbf{s}^{-2} \mathbf{s} \cdot \mathbf{n} \mathbf{s}, \quad \mathcal{Y}_{lm}(\mathbf{x}) = |\mathbf{x}|^l Y_{lm}(\hat{\mathbf{x}})$$

$$F_0(x) = -1 + \frac{1}{2} \int_0^1 dt \frac{e^{tx} - 1}{t^{3/2}}$$

- choose $\Lambda \approx 1$ for convergence of the summation
- integral done Gauss-Legendre quadrature
- $F_0(x)$ given in terms of Dawson or erf function

K matrix

- quantization condition relates single energy E to entire S -matrix
- cannot solve for S -matrix (except single channel, single wave)
- approximate S -matrix with functions depending on handful of fit parameters
- obtain estimates of fit parameters using many energies
- easier to parametrize Hermitian matrix than unitary matrix
- introduce K -matrix (Wigner 1946)

$$S = (1 + iK)(1 - iK)^{-1} = (1 - iK)^{-1}(1 + iK)$$

- Hermiticity of K -matrix ensures unitarity of S -matrix
- with time reversal invariance, K -matrix must be real and symmetric

K matrix

- multichannel effective range expansion (Ross 1961)

$$K_{L'S'a'; L'Sa}^{-1}(E) = q_{a'}^{-L'-\frac{1}{2}} \tilde{K}_{L'S'a'; L'Sa}^{-1}(E_{\text{cm}}) q_a^{-L-\frac{1}{2}},$$

- quantization condition can be written

$$\det(1 - B^{(P)} \tilde{K}) = \det(1 - \tilde{K} B^{(P)}) = 0$$

- we define the **box matrix** by

$$\begin{aligned} \langle J'm_J L'S'a' | B^{(P)} | Jm_J L'Sa \rangle &= -i \delta_{a'a} \delta_{S'S} u_a^{L'+L+1} W_{L'm_{L'}; Lm_L}^{(Pa)} \\ &\times \langle J'm_J | L'm_{L'}, S m_S \rangle \langle Lm_L, S m_S | Jm_J \rangle \end{aligned}$$

- box matrix is **Hermitian** for u_a^2 real
- quantization condition can also be expressed as

$$\det(\tilde{K}^{-1} - B^{(P)}) = 0$$

- these determinants are **real**

Block diagonalization

- quantization condition involves determinant of infinite matrix
- make practical by (a) transforming to a block-diagonal basis and (b) truncating in orbital angular momentum
- block-diagonal basis

$$|\Lambda\lambda n J L S a\rangle = \sum_{m_J} c_{m_J}^{J(-1)^L; \Lambda\lambda n} |J m_J L S a\rangle$$

- little group irrep Λ , irrep row λ , occurrence index n
- transformation coefficients depend on J and $(-1)^L$, not on S, a
- replaces m_J by (Λ, λ, n)
- group theoretical projections with Gram-Schmidt used to obtain coefficients
- use notation and irrep matrices from PRD 88, 014511 (2013)

Box and \tilde{K} matrices in block diagonal basis

- in block-diagonal basis, box matrix has form

$$\langle \Lambda' \lambda' n' J' L' S' a' | B^{(P)} | \Lambda \lambda n J L S a \rangle = \delta_{\Lambda' \Lambda} \delta_{\lambda' \lambda} \delta_{S' S} \delta_{a' a} B_{J' L' n'; J L n}^{(P \Lambda_B S a)}(E)$$

- \tilde{K} -matrix for $(-1)^{L+L'} = 1$ has form

$$\langle \Lambda' \lambda' n' J' L' S' a' | \tilde{K} | \Lambda \lambda n J L S a \rangle = \delta_{\Lambda' \Lambda} \delta_{\lambda' \lambda} \delta_{n' n} \delta_{J' J} \mathcal{K}_{L' S' a'; L S a}^{(J)}(E_{\text{cm}})$$

- $(-1)^{L+L'} = 1 \Rightarrow \eta_{1a'}^P \eta_{2a'}^P = \eta_{1a}^P \eta_{2a}^P$, always applies in QCD
- Λ is irrep for K -matrix, need Λ_B for box matrix
- when $\eta_{1a}^P \eta_{2a}^P = 1$, then $\Lambda_B = \Lambda$

d	LG	Λ_B relationship to Λ when $\eta_{1a}^P \eta_{2a}^P = -1$
$(0, 0, 0)$	O_h	Subscript $g \leftrightarrow u$
$(0, 0, n)$	C_{4v}	$A_1 \leftrightarrow A_2$; $B_1 \leftrightarrow B_2$; E, G_1, G_2 stay same
$(0, n, n)$	C_{2v}	$A_1 \leftrightarrow A_2$; $B_1 \leftrightarrow B_2$; G stays same
(n, n, n)	C_{3v}	$A_1 \leftrightarrow A_2$; $F_1 \leftrightarrow F_2$; E, G stay same

- see PRD 88, 014511 (2013) for notation

K matrix parametrizations

- \tilde{K} matrix in block diagonal basis

$$\langle \Lambda' \lambda' n' J' L' S' a' | \tilde{K} | \Lambda \lambda n J L S a \rangle = \delta_{\Lambda' \Lambda} \delta_{\lambda' \lambda} \delta_{n' n} \delta_{J' J} \mathcal{K}_{L' S' a'; L S a}^{(J)}(E_{\text{cm}})$$

$$\langle \Lambda' \lambda' n' J' L' S' a' | \tilde{K}^{-1} | \Lambda \lambda n J L S a \rangle = \delta_{\Lambda' \Lambda} \delta_{\lambda' \lambda} \delta_{n' n} \delta_{J' J} \mathcal{K}_{L' S' a'; L S a}^{(J)-1}(E_{\text{cm}})$$

- common parametrization

$$\mathcal{K}_{\alpha\beta}^{(J)-1}(E_{\text{cm}}) = \sum_{k=0}^{N_{\alpha\beta}} c_{\alpha\beta}^{(Jk)} E_{\text{cm}}^k$$

- α, β compound indices for (L, S, a)
- another common parametrization

$$\mathcal{K}_{\alpha\beta}^{(J)}(E_{\text{cm}}) = \sum_p \frac{g_{\alpha}^{(Jp)} g_{\beta}^{(Jp)}}{E_{\text{cm}}^2 - m_{Jp}^2} + \sum_k d_{\alpha\beta}^{(Jk)} E_{\text{cm}}^k,$$

- Lorentz invariant form using $E_{\text{cm}} = \sqrt{s}$
- Mandelstam variable $s = (p_1 + p_2)^2$, with p_j four-momentum of particle j

Box matrix elements

- have obtained expressions for $B_{J'L'n'; JLn}^{(P\Lambda_B S_a)}(E)$ for
- $L \leq 6, S \leq 2$ with $\mathbf{P} = (0, 0, 0), (0, 0, p), p > 0$
- $L \leq 6, S \leq \frac{3}{2}$ with $\mathbf{P} = (0, p, p), (p, p, p), p > 0$
- in tables that follow, we define

R_{lm} is short hand for $(\gamma\pi^{3/2}u_a^{l+1})^{-1}\text{Re } \mathcal{Z}_{lm}(\mathbf{s}_a, \gamma, u_a^2)$

I_{lm} is short hand for $(\gamma\pi^{3/2}u_a^{l+1})^{-1}\text{Im } \mathcal{Z}_{lm}(\mathbf{s}_a, \gamma, u_a^2)$

- C++ software available on github: [TwoHadronsInBox](#)

Box matrix elements $P = 0, S = 0$

J'	L'	n'	J	L	n	$u_a^{-(L'+L+1)} B$
$\Lambda_B = A_{1g}$						
0	0	1	0	0	1	R_{00}
0	0	1	4	4	1	$\frac{2\sqrt{21}}{7} R_{40}$
0	0	1	6	6	1	$-2\sqrt{2} R_{60}$
4	4	1	4	4	1	$R_{00} + \frac{108}{143} R_{40} + \frac{80\sqrt{13}}{143} R_{60} + \frac{560\sqrt{17}}{2431} R_{80}$
4	4	1	6	6	1	$-\frac{40\sqrt{546}}{1001} R_{40} + \frac{42\sqrt{42}}{187} R_{60} - \frac{224\sqrt{9282}}{46189} R_{80} - \frac{1008\sqrt{26}}{4199} R_{10,0}$
6	6	1	6	6	1	$R_{00} - \frac{126}{187} R_{40} - \frac{160\sqrt{13}}{3553} R_{60} + \frac{840\sqrt{17}}{3553} R_{80} - \frac{2016\sqrt{21}}{7429} R_{10,0}$ $+ \frac{30492}{37145} R_{12,0} - \frac{1848\sqrt{1001}}{37145} R_{12,4}$
$\Lambda_B = A_{2g}$						
6	6	1	6	6	1	$R_{00} + \frac{6}{17} R_{40} - \frac{160\sqrt{13}}{323} R_{60} - \frac{40\sqrt{17}}{323} R_{80} - \frac{2592\sqrt{21}}{7429} R_{10,0}$ $+ \frac{1980}{7429} R_{12,0} + \frac{264\sqrt{1001}}{7429} R_{12,4}$
$\Lambda_B = A_{2u}$						
3	3	1	3	3	1	$R_{00} - \frac{12}{11} R_{40} + \frac{80\sqrt{13}}{143} R_{60}$

Box matrix elements $P = 0, S = 0$

J'	L'	n'	J	L	n	$u_a^{-(L'+L+1)} B$
$\Lambda_B = E_g$						
2	2	1	2	2	1	$R_{00} + \frac{6}{7} R_{40}$
2	2	1	4	4	1	$-\frac{40\sqrt{3}}{77} R_{40} - \frac{30\sqrt{39}}{143} R_{60}$
2	2	1	6	6	1	$\frac{30\sqrt{910}}{1001} R_{40} + \frac{4\sqrt{70}}{55} R_{60} + \frac{8\sqrt{15470}}{1105} R_{80}$
4	4	1	4	4	1	$R_{00} + \frac{108}{1001} R_{40} - \frac{64\sqrt{13}}{143} R_{60} + \frac{392\sqrt{17}}{2431} R_{80}$
4	4	1	6	6	1	$-\frac{8\sqrt{2730}}{1001} R_{40} - \frac{18\sqrt{210}}{187} R_{60} - \frac{128\sqrt{46410}}{46189} R_{80}$ $-\frac{1512\sqrt{130}}{20995} R_{10,0}$
6	6	1	6	6	1	$R_{00} + \frac{114}{187} R_{40} + \frac{480\sqrt{13}}{3553} R_{60} + \frac{280\sqrt{17}}{3553} R_{80} + \frac{1152\sqrt{21}}{7429} R_{10,0}$ $+ \frac{30492}{37145} R_{12,0} + \frac{264\sqrt{1001}}{37145} R_{12,4}$
$\Lambda_B = E_u$						
5	5	1	5	5	1	$R_{00} - \frac{6}{13} R_{40} + \frac{32\sqrt{13}}{221} R_{60} - \frac{672\sqrt{17}}{4199} R_{80} + \frac{1152\sqrt{21}}{4199} R_{10,0}$
$\Lambda_B = T_{1g}$						
4	4	1	4	4	1	$R_{00} + \frac{54}{143} R_{40} - \frac{4\sqrt{13}}{143} R_{60} - \frac{448\sqrt{17}}{2431} R_{80}$
4	4	1	6	6	1	$-\frac{12\sqrt{65}}{143} R_{40} + \frac{42\sqrt{5}}{187} R_{60} + \frac{112\sqrt{1105}}{46189} R_{80} + \frac{576\sqrt{1365}}{20995} R_{10,0}$
6	6	1	6	6	1	$R_{00} - \frac{96}{187} R_{40} - \frac{80\sqrt{13}}{3553} R_{60} + \frac{120\sqrt{17}}{3553} R_{80} + \frac{624\sqrt{21}}{7429} R_{10,0}$ $-\frac{26136}{37145} R_{12,0} + \frac{1584\sqrt{1001}}{37145} R_{12,4}$

Box matrix elements $P = (2\pi/L)(0, n, n)$, $S = \frac{1}{2}$

J'	L'	n'	J	L	n	$u_a^{-(L'+L+1)} B$
$\Lambda_B = G$ (partial)						
$\frac{5}{2}$	2	2	$\frac{9}{2}$	5	4	$-\frac{3\sqrt{105}}{308}iR_{30} - \frac{13\sqrt{14}}{924}iR_{32} - \frac{7\sqrt{165}}{286}iR_{50} + \frac{95\sqrt{154}}{3003}iR_{52}$ $-\frac{25\sqrt{462}}{2002}iR_{54} + \frac{915}{2288}iR_{70} + \frac{375\sqrt{21}}{16016}iR_{72}$ $-\frac{675\sqrt{462}}{16016}iR_{74} + \frac{15\sqrt{3003}}{2288}iR_{76}$
$\frac{5}{2}$	2	2	$\frac{9}{2}$	5	5	$-\frac{23\sqrt{30}}{924}R_{30} - \frac{95}{462}R_{32} - \frac{2\sqrt{2310}}{3003}R_{50} + \frac{2\sqrt{11}}{429}R_{52}$ $+\frac{16\sqrt{33}}{429}R_{54} + \frac{135\sqrt{14}}{2288}R_{70} + \frac{435\sqrt{6}}{2288}R_{72}$ $+\frac{105\sqrt{33}}{1144}R_{74} + \frac{45\sqrt{858}}{2288}R_{76}$
$\frac{5}{2}$	2	2	$\frac{11}{2}$	5	1	$\frac{\sqrt{105}}{13}R_{54} - \frac{\sqrt{105}}{65}R_{74} - \frac{\sqrt{2730}}{455}R_{76}$
	2	2	$\frac{11}{2}$	5	2	$-\frac{5\sqrt{35}}{77}R_{32} + \frac{10\sqrt{385}}{1001}R_{52} - \frac{\sqrt{1155}}{1001}R_{54} - \frac{5\sqrt{210}}{2002}R_{72}$ $+\frac{2\sqrt{1155}}{715}R_{74} + \frac{3\sqrt{30030}}{1430}R_{76}$
$\frac{5}{2}$	2	2	$\frac{11}{2}$	5	3	$-\frac{5\sqrt{70}}{231}R_{30} + \frac{10\sqrt{21}}{231}R_{32} + \frac{10\sqrt{110}}{429}R_{50} + \frac{2\sqrt{231}}{273}R_{52}$ $-\frac{\sqrt{77}}{13}R_{54} - \frac{5\sqrt{6}}{143}R_{70} + \frac{27\sqrt{14}}{1001}R_{72} - \frac{3\sqrt{77}}{143}R_{74}$
$\frac{5}{2}$	2	2	$\frac{11}{2}$	5	4	$\frac{5\sqrt{7}}{11}R_{32} + \frac{8\sqrt{77}}{143}R_{52} - \frac{9\sqrt{231}}{1001}R_{54} - \frac{17\sqrt{42}}{286}R_{72}$ $-\frac{6\sqrt{231}}{1001}R_{74} - \frac{5\sqrt{6006}}{2002}R_{76}$
$\frac{5}{2}$	2	2	$\frac{11}{2}$	5	5	$\frac{5\sqrt{35}}{33}R_{30} + \frac{5\sqrt{42}}{231}R_{32} - \frac{7\sqrt{55}}{429}R_{50} - \frac{\sqrt{462}}{3003}R_{52}$ $+\frac{10\sqrt{154}}{1001}R_{54} - \frac{42\sqrt{3}}{143}R_{70} - \frac{6\sqrt{7}}{1001}R_{72} - \frac{15\sqrt{154}}{1001}R_{74}$
$\frac{5}{2}$	2	2	$\frac{11}{2}$	5	6	$\frac{50}{231}iR_{30} + \frac{5\sqrt{30}}{77}iR_{32} + \frac{5\sqrt{77}}{429}iR_{50} - \frac{3\sqrt{330}}{143}iR_{52}$ $+\frac{4\sqrt{105}}{715}iR_{70} - \frac{192\sqrt{5}}{715}iR_{72}$

Fitting: spectrum method

- adjust K -matrix parameters to reproduce energies from lattice QCD
- choose $E_{\text{cm},k}$ as observables
- model predictions by solving quantization for κ_j parameters
- problems:
 - root finding difficult, many computations of RGL zeta functions
 - ambiguity mapping model energies to observed energies
 - model predictions depend on observables m_{1a} , m_{2a} , L , ξ so must recompute covariance during minimization
- “Lagrange multiplier” trick removes obs. dependence in model
 - include m_{1a} , m_{2a} , L , ξ as both observables and model parameters
- observations

$$\text{Observations } R_i: \{ E_{\text{cm},k}^{(\text{obs})}, m_j^{(\text{obs})}, L^{(\text{obs})}, \xi^{(\text{obs})} \},$$

- model parameters

$$\text{Model fit parameters } \alpha_k: \{ \kappa_i, m_j^{(\text{model})}, L^{(\text{model})}, \xi^{(\text{model})} \},$$

Fitting: spectrum method (con't)

- residuals

$$r_k = \begin{cases} E_{\text{cm},k}^{(\text{obs})} - E_{\text{cm},k}^{(\text{model})}, & (k = 1, \dots, N_E), \\ m_{k'}^{(\text{obs})} - m_{k'}^{(\text{model})}, & (k = k' + N_E, k' = 1, \dots, N_p), \\ L^{(\text{obs})} - L^{(\text{model})}, & (k = N_E + N_p + 1), \\ \xi^{(\text{obs})} - \xi^{(\text{model})}, & (k = N_E + N_p + 2). \end{cases}$$

- compute $E_{\text{cm},k}^{(\text{model})}$ using only model parameters
- emphasize $E_{\text{cm},k}^{(\text{model})}$ very difficult to compute

Fitting: determinant residual method

- introduce quantization determinant as residual
- better to use function of matrix A with real parameter μ :

$$\Omega(\mu, A) \equiv \frac{\det(A)}{\det[(\mu^2 + AA^\dagger)^{1/2}]}$$

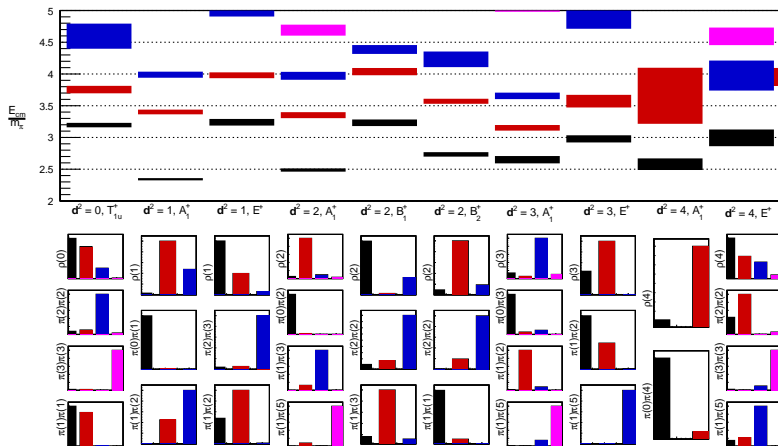
- evaluated using only eigenvalues; role of μ to suppress contributions from irrelevant higher-lying eigenvalues
- residuals

$$r_k = \Omega\left(\mu, 1 - B^{(\mathbf{P})}(E_{\text{cm},k}^{(\text{obs})}) \tilde{K}(E_{\text{cm},k}^{(\text{obs})})\right), \quad (k = 1, \dots, N_E),$$

- use only **observed** energies, particle masses, lattice size, anisotropy
- advantage: model predictions do not need root finding or RGL zeta computations
- model depends on observables, so covariance must be recomputed as κ_j parameters adjusted during minimization
- covariance recomputation still **much** simpler than root finding required in spectrum method

$\pi\pi$ $I = 1$ energies in finite volume

- finite volume energies $32^3 \times 256$ lattice, $m_\pi \approx 240$ MeV



Decay width of ρ

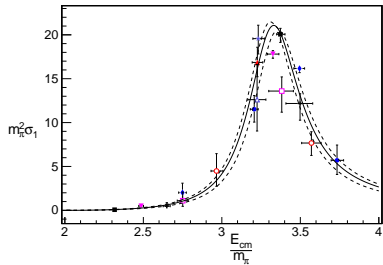
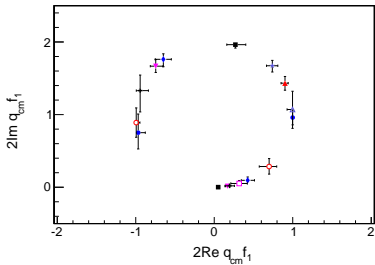
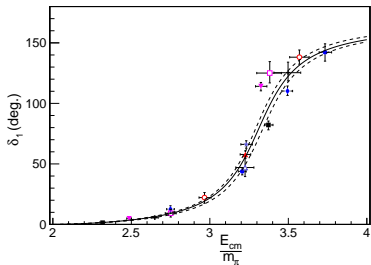
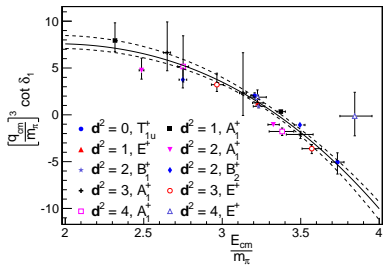
- applied to $I = 1 \rho \rightarrow \pi\pi$ system NPB 910, 842 (2016)
- included $L = 1, 3, 5$ partial waves in NPB 924, 477 (2017)
- large $32^3 \times 256$ anisotropic lattice, $m_\pi \approx 240$ MeV
- fit forms (first ever inclusion of $L = 5$ in lattice QCD):

$$(\tilde{K}^{-1})_{11} = \frac{6\pi E_{\text{cm}}}{g^2 m_\pi} \left(\frac{m_\rho^2}{m_\pi^2} - \frac{E_{\text{cm}}^2}{m_\pi^2} \right)$$
$$(\tilde{K}^{-1})_{33} = \frac{1}{m_\pi^7 a_3} \quad (\tilde{K}^{-1})_{55} = \frac{1}{m_\pi^{11} a_5}$$

- results

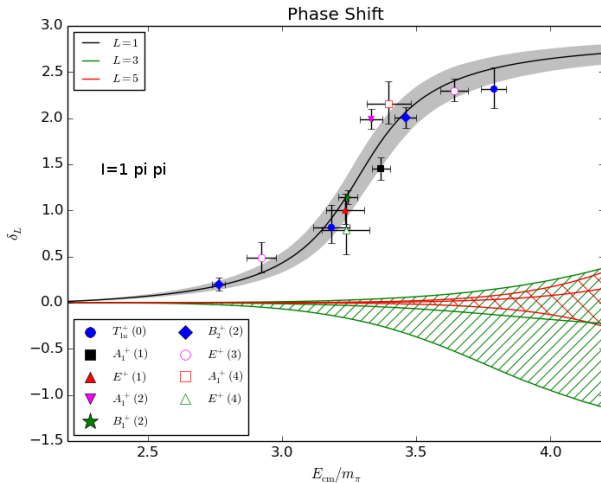
$$\frac{m_\rho}{m_\pi} = 3.349(25), \quad g = 5.97(27), \quad m_\pi^7 a_3 = -0.00021(100),$$
$$m_\pi^{11} a_5 = -0.00006(24), \quad \chi^2/\text{dof} = 1.15$$

Decay of ρ



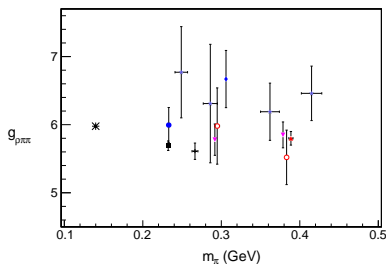
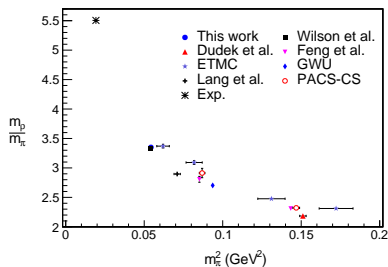
Decay of ρ

- plot of phase shifts



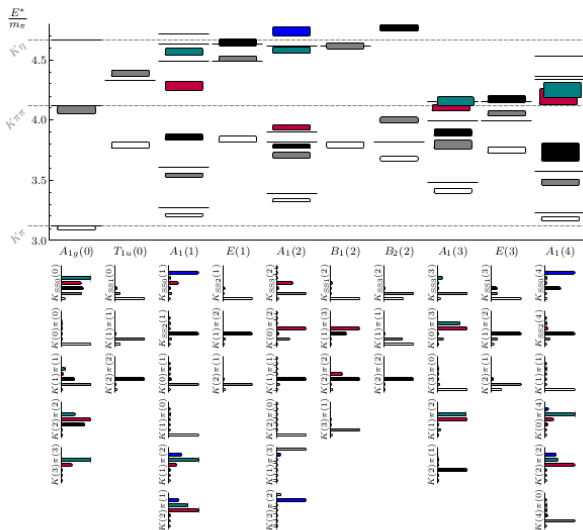
Comparison to other works

- comparison of our m_ρ and $g_{\rho\pi\pi}$ to other works



$K\pi$ energies in finite volume

- finite volume energies $32^3 \times 256$ lattice, $m_\pi \approx 240$ MeV



Decay of K^* (892)

- studied $K^*(892)$
- included $L = 0, 1, 2$ partial waves
- large $32^3 \times 256$ anisotropic lattice, $m_\pi \approx 240$ MeV
- fit forms

$$(\tilde{K}^{-1})_{11} = \frac{6\pi E_{\text{cm}}}{g_{K^*\pi\pi}^2 m_\pi} \left(\frac{m_{K^*}^2}{m_\pi^2} - \frac{E_{\text{cm}}^2}{m_\pi^2} \right) \quad (\tilde{K}^{-1})_{22} = \frac{-1}{m_\pi^5 a_2}$$

- S -wave forms tried:

$$\begin{aligned}(\tilde{K}^{-1})_{00}^{\text{lin}} &= a_1 + b_1 E_{\text{cm}}, \\(\tilde{K}^{-1})_{00}^{\text{quad}} &= a_q + b_q E_{\text{cm}}^2, \\(\tilde{K}^{-1})_{00}^{\text{ERE}} &= \frac{-1}{m_\pi a_0} + \frac{m_\pi r_0}{2} \frac{q_{\text{cm}}^2}{m_\pi^2}, \\(\tilde{K}^{-1})_{00}^{\text{BW}} &= \left(\frac{m_{K_0^*}^2}{m_\pi^2} - \frac{E_{\text{cm}}^2}{m_\pi^2} \right) \frac{6\pi m_\pi E_{\text{cm}}}{g_{K_0^*\pi\pi}^2 m_{K_0^*}^2}\end{aligned}$$

K -matrix fits

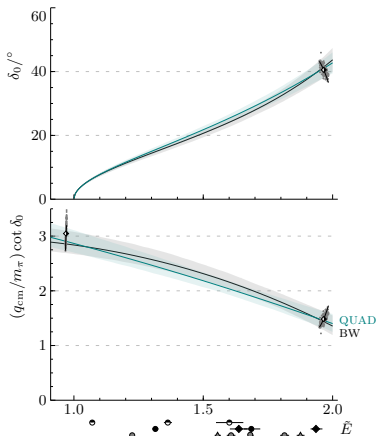
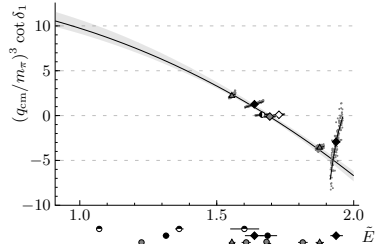
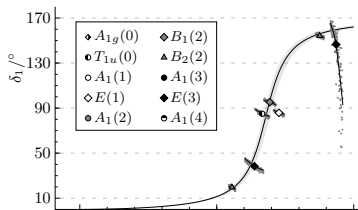
- summary of fit results

Fit	s -wave par.	m_{K^*}/m_π	$g_{K^*K\pi}$	$m_\pi a_0$	$\chi^2/\text{d.o.f.}$
(1a,1b)	LIN	3.819(20)	5.54(25)	-0.333(31)	(1.04,-)
2	LIN	3.810(18)	5.30(19)	-0.349(25)	1.49
3	QUAD	3.810(18)	5.31(19)	-0.350(25)	1.47
4	ERE	3.809(17)	5.31(20)	-0.351(24)	1.47
5	BW	3.808(18)	5.33(20)	-0.353(25)	1.42
6	BW	3.810(17)	5.33(20)	-0.354(25)	1.50

- $q\bar{q}$ operators in $A_{1g}(0)$ channel overlap many eigenvectors
- better energy resolution needed for $K_0^*(800)$ determination (future work)
- from NLO effective range parametrization find $m_R/m_\pi = 4.66(13) - 0.87(18)i$ (consistent with BW fit)

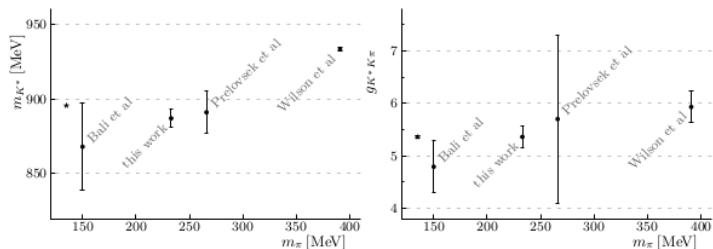
Decay of $K^*(892)$

- plot of P -wave and S -wave phase shift
- included $L = 0, 1, 2$ partial waves
- large $32^3 \times 256$ anisotropic lattice, $m_\pi \approx 240$ MeV
- κ fit: quadratic



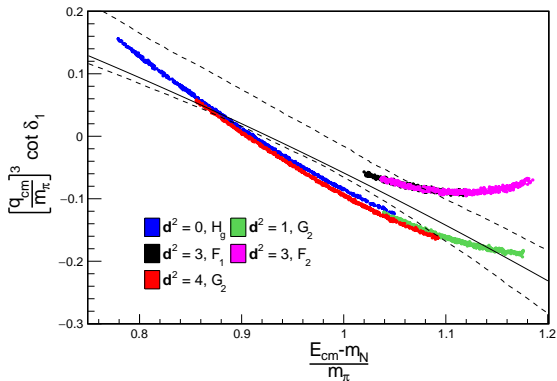
Comparison to other works

- comparison of our m_{K^*} and $g_{K^*K\pi}$ to other works



Decay of Δ

- first baryon resonance decay study
- included $L = 1$ wave only (for now) PRD **97**, 014506 (2018)
- large $48^3 \times 128$ isotropic lattice, $m_\pi \approx 280$ MeV, $a \sim 0.076$ fm
- Breit-Wigner fit gives $g_{\Delta N \pi} = 19.0(4.7)$ in agreement with experiment ~ 16.9



Recent $I = 1$ $\pi\pi$ scattering results

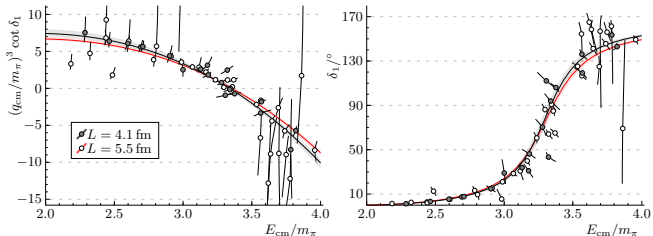
- Most recent work on CLS ensembles NPB939, 145 (2019)

ID	a [fm]	$L^3 \times T$	m_π, m_K [MeV]	N_{conf}
C101	0.086	$48^3 \times 96$	220, 470	300
D101		$64^3 \times 128$		303
N401	0.076	$48^3 \times 128$	280, 460	274
N200	0.064	$48^3 \times 128$	280, 460	854
D200		$64^3 \times 128$	200, 480	558
J303	0.050	$64^3 \times 192$	260, 470	328

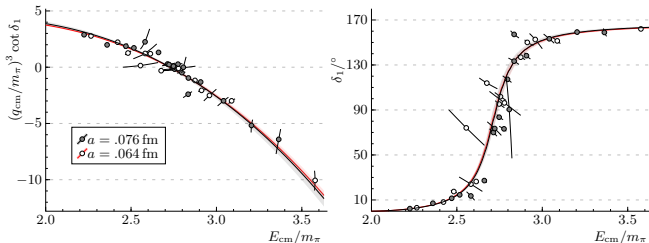
ID	(ρ, n_ρ)	N_{ev}	dilution	N_{t_0}	N_{inv}
C101	(0.1, 20)	392	(TF, SF, LI16) _F (TI8, SF, LI16) _R	1	1408
D101		928	(TF, SF, LI16) _F (TI8, SF, LI16) _R	2	1792
N401	(0.1, 25)	320	(TF, SF, LI16) _F (TI8, SF, LI16) _R	2	1664
N200	(0.1, 36)	192	(TF, SF, LI8) _F (TI8, SF, LI8) _R	2	832
D200		448	(TF, SF, LI8) _F (TI8, SF, LI8) _R	2	832
J303	(0.1, 60)	208	(TF, SF, LI8) _F (TI16, SF, LI8) _R	3	1504

Decay of the ρ

- scattering phase shift for C101 and D101

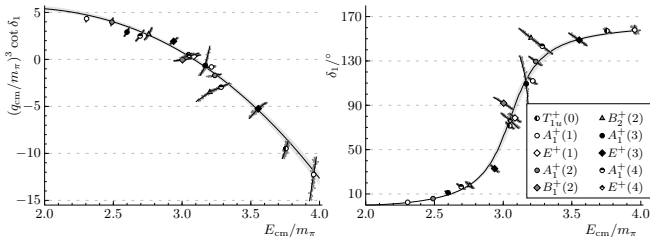


- scattering phase shift for N200 and N401

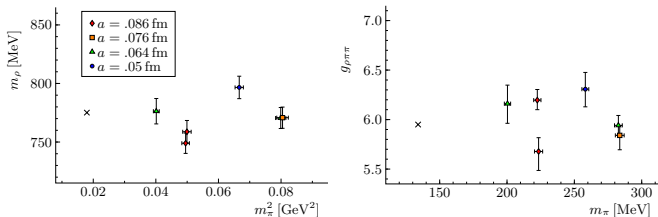


Decay of the ρ

- scattering phase shift for J303



- summary of resonance parameters



Time-like pion form factor

- obtain time-like pion form factor NPB**939**, 145 (2019) from

$$|F_\pi(E_{\text{cm}})|^2 = g_\Lambda(\gamma) \left(q_{\text{cm}} \frac{\partial \delta_1}{\partial q_{\text{cm}}} + u \frac{\partial \phi_1^{(\mathbf{d}, \Lambda)}}{\partial u} \right) \frac{3\pi E_{\text{cm}}^2}{2q_{\text{cm}}^5 L^3} |\langle 0 | V^{(\mathbf{d}, \Lambda)} | \mathbf{d} \Lambda n \rangle|^2$$

where

$$\gamma = \frac{E}{E_{\text{cm}}}, \quad u = \frac{Lq_{\text{cm}}}{2\pi}, \quad g_\Lambda(\gamma) = \begin{cases} \gamma^{-1}, & \Lambda = A_1^+ \\ \gamma, & \text{otherwise} \end{cases}$$

and δ_1 is the physical phase shift, and

$B_{11}^{(\mathbf{d}, \Lambda)} = (q_{\text{cm}}/m_\pi)^3 \cot \phi_1^{(\mathbf{d}, \Lambda)}$ gives the pseudophase $\phi_1^{(\mathbf{d}, \Lambda)}$

- we compute the matrix element

$$V^{(\mathbf{d}, \Lambda)} = \sum_\mu b_\mu^{(\mathbf{d}, \Lambda)} V_{R, \mu}, \quad \sum_\mu b_\mu^{(\mathbf{d}, \Lambda)*} b_\mu^{(\mathbf{d}, \Lambda)} = 1,$$

$$V_{R, \mu} = Z_V (1 + ab_V m_1 + a\bar{b}_V \text{Tr} M_q) V_{I, \mu}, \quad V_{I, \mu} = V_\mu + ac_V \tilde{\partial}_\nu T_{\mu\nu},$$

$$V_\mu^a = \frac{1}{2} \bar{\psi} \gamma_\mu \tau^a \psi, \quad \tilde{\partial}_\nu T_{\mu\nu}^a = \frac{1}{2} i \tilde{\partial}_\nu \bar{\psi} \sigma_{\mu\nu} \tau^a \psi$$

Time-like pion form factor (con't)

- renormalization constants determined nonperturbatively
- tried Gounaris-Sakurai parametrization

$$F_{\pi}^{GS}(\sqrt{s}) = \frac{-\frac{m_{\pi}^2}{\pi} - q_{\rho}^2 h(m_{\rho}) - b \frac{m_{\rho}^2}{4}}{q_{\text{cm}}^2 h(\sqrt{s}) - q_{\rho}^2 h(m_{\rho}) + b(q_{\text{cm}}^2 - q_{\rho}^2) - \frac{q_{\text{cm}}^3}{\sqrt{s}} i},$$

$$b = -h(m_{\rho}) - \frac{24\pi}{g_{\rho\pi\pi}^2} - \frac{2q_{\rho}^2}{m_{\rho}} h'(m_{\rho}),$$

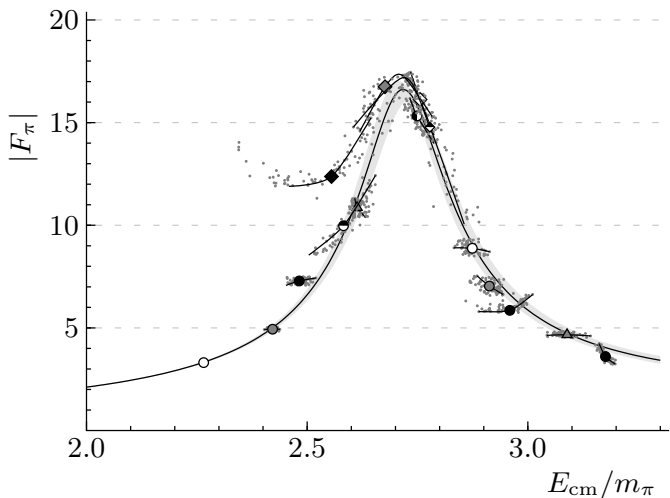
$$h(\sqrt{s}) = \frac{2}{\pi} \frac{q_{\text{cm}}}{\sqrt{s}} \ln \left(\frac{\sqrt{s} + 2q_{\text{cm}}}{2m_{\pi}} \right),$$

- also tried n -subtracted dispersion relation with Omnes-Muskhelishvili solution

$$F_{\pi}(s) = \exp \left(\sum_{k=1}^n p_k s^k \right) \exp \left\{ \frac{s^n}{\pi} \int_{4m_{\pi}^2}^{\infty} \frac{dz}{z^n} \frac{\delta_1(z)}{z - s - i\epsilon} \right\}$$

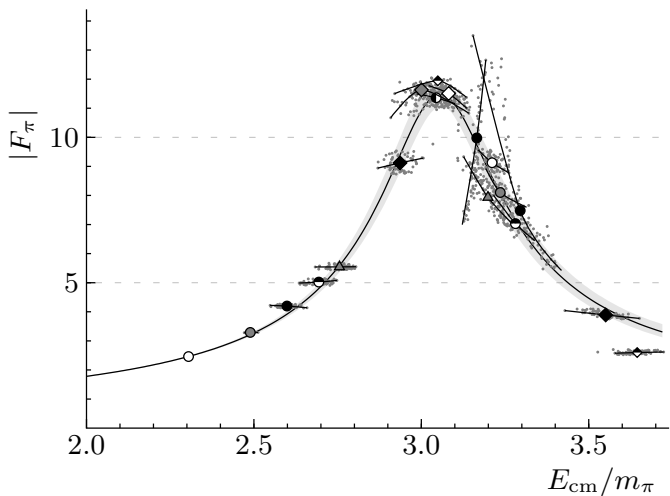
Time-like pion form factor results

- results for N200 (curve is fit with thrice-subtracted dispersion)



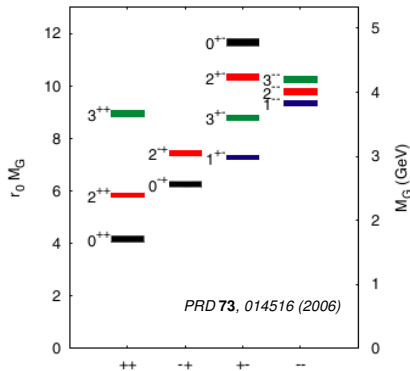
Time-like pion form factor results

- results for J303 (curve is fit with thrice-subtracted dispersion)

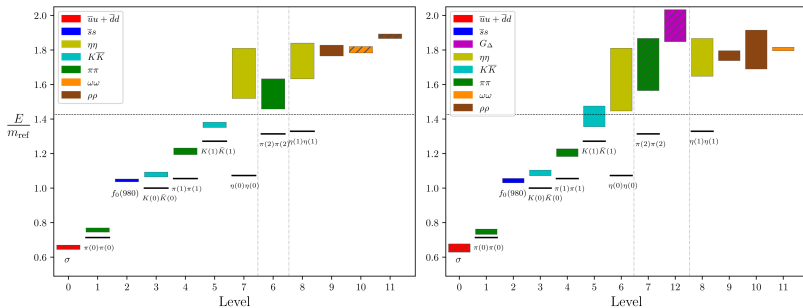


The scalar glueball

- glueball: hypothetical bound state of gluons
- experimental evidence elusive, light scalar candidates:
 - $f_0(1370)$, $f_0(1500)$, $f_0(1710)$
- lattice studies to date:
 - light scalar $\sim 1600 - 1700$ MeV
 - most in pure $SU(3)$ or quenched approx. (no quark/meson mixing!)
- here: extract low-lying A_{1g}^+ spectrum with $q\bar{q}$, meson-meson, & glueball operators
 - first look (from the lattice) at mixing between glueball, $q\bar{q}$, and two-hadron states

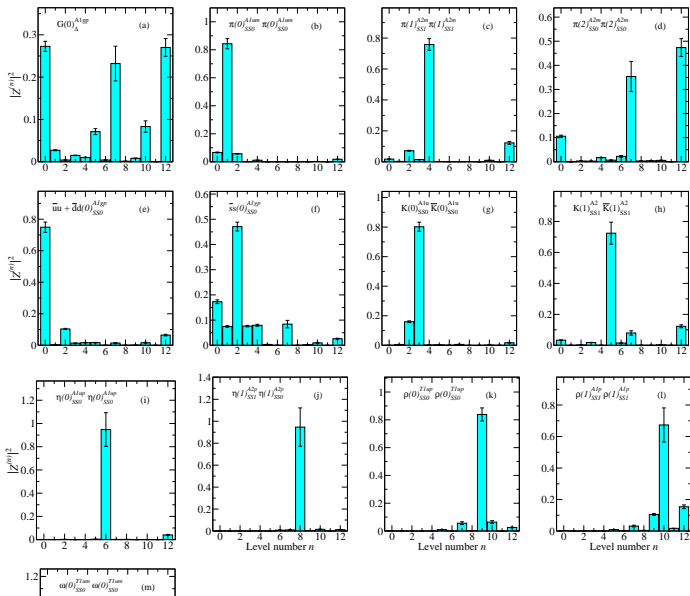


- $24^3 \times 128$ anisotropic lattice, $m_\pi \sim 390$ MeV



- bad news for the scalar glueball?

A_{1g}^+ overlaps



Tetraquark operators

- determine impact on spectrum when tetraquark operators included
- tetraquark operators we study are combinations of

$$\Phi_{\alpha\beta\mu\nu;ijkl}^{ABCD\pm}(t) = \sum_{\mathbf{x}} e^{-i\mathbf{p}\cdot\mathbf{x}} (\delta_{ab}\delta_{cd} \pm \delta_{ad}\delta_{bc}) \bar{q}_{a\alpha i}^A(\mathbf{x}, t) q_{b\beta j}^B(\mathbf{x}, t) \bar{q}_{c\mu k}^C(\mathbf{x}, t) q_{d\nu l}^D(\mathbf{x}, t),$$



SS



DD1a



DD1b



QDXa

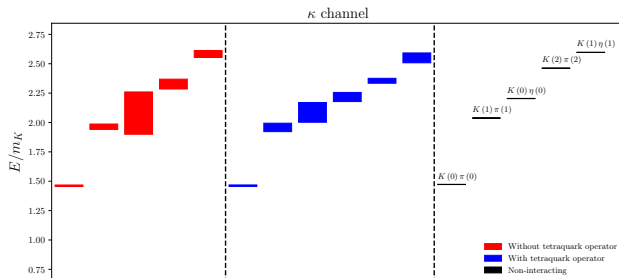


QDXb

- spectrum in κ , $a_0(980)$ channels using $32^3 \times 256$ anisotropic lattice $m_\pi \approx 235$ MeV, $N_{\text{cfgs}} = 412$, $\xi \approx 3.451$.

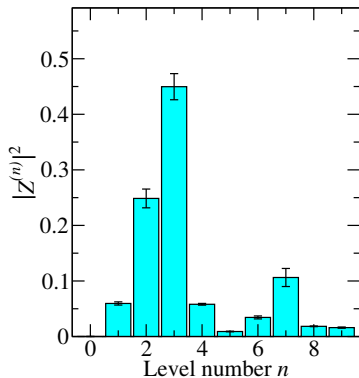
$I = \frac{1}{2}, S = 1, A_{1g}$ channel for $K_0^*(700)$

- single-site and displaced $q\bar{q}$, $K\pi$, $K\phi$, and $K\eta$ operators
- tried several hundred tetraquark operators, different flavor structures
- found a dozen or so operators yield additional energy level
- never got two extra levels



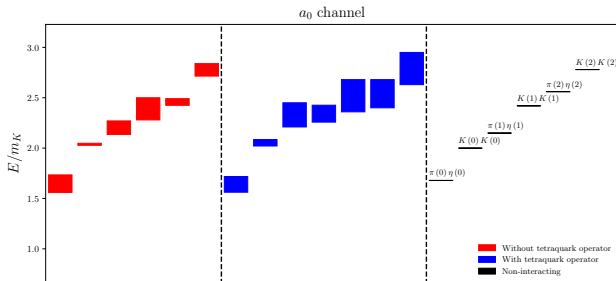
$I = \frac{1}{2}, S = 1, A_{1g}$ channel for $K_0^*(700)$ (con't)

- Overlap factors for single-site $\bar{s}u\bar{s}s$ color antisym tetraquark operator



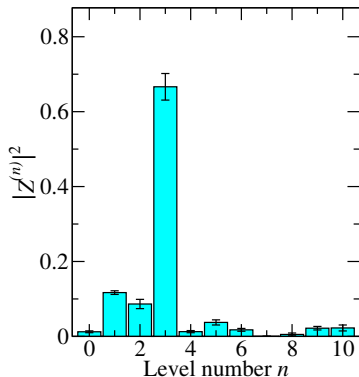
$I = 1, S = 0, A_{1g}^-$ channel for $a_0(980)$

- single-site and displaced $q\bar{q}$, $K\bar{K}$, $\eta\pi$, and $\phi\pi$ operators
- tried several hundred tetraquark operators, different flavor structures
- found a dozen or so operators yield additional energy level
- never got two extra levels



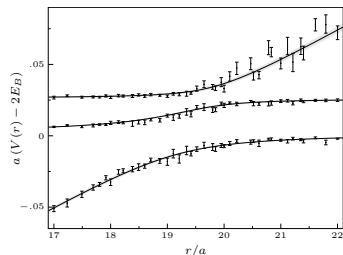
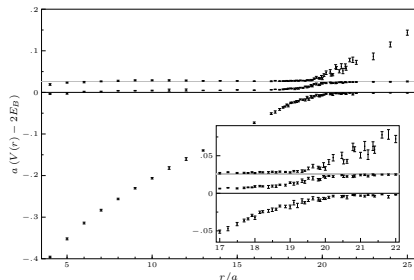
$I = 1, S = 0, A_{1g}^-$ channel for $a_0(980)$ (con't)

- Overlap factors for single-site $\bar{u}u\bar{d}s$ color antisym tetraquark operator



String Breaking

- string breaking (with Vanessa Koch et al.) PLB 793, 493 (2019)
- Wilson line operator with static-light $B\bar{B}$ and $B_s\bar{B}_s$ operators
- use of stochastic LapH method
- $N_f = 2 + 1$ CLS N200 ensemble $48^3 \times 128$, $a = 0.064$ fm, $m_\pi 280$ MeV, $m_K = 460$ MeV



Collaborators

- people involved in this work:



John Bulava
U. of S. Denmark



Ruairi Brett
GWU



Daniel Darvish
CMU



Jake Fallica
U. Kentucky,
Lexington



Andrew Hanlon
University of Mainz



Ben Hörz
Lawrence Berkeley



Christian Walther
Andersen
U. of S. Denmark

- thanks to NSF XSEDE:

- Stampede at TACC
- Comet at SDSC



Current Efforts

- recently joined with CalLat (Walker-Loud and others) and U. Mainz (Wittig and others) to study baryon-baryon scattering
- major software redevelopment: common subexpression elimination with tensor contractions, heavy use of batched BLAS routines (with Ben Hörz)
- DOE INCITE award on Summit at ORNL
- large volumes near physical point
- NN , $N\Sigma$, $N\Lambda$, $\Lambda\Lambda$, $N\Xi$ included
- also includes $N\bar{K}$, $N\pi$, $\Sigma\pi$
- $\Lambda(1405)$, $\Delta(1232)$, H -dibaryon, and Roper to be studied
- Δ transition form factors

Proton mass decomposition

- recent determination of mass decomposition of proton
[Y.Yang, J.Liang, Y.Bi, Y.Chen, T.Draper, K.F.Liu, Z.Liu, PRL121, 212001 (2018)]
- rest mass M of proton given by [Ji PRL74, 1071 (1995)]

$$M = -\langle T_{44} \rangle = \langle H_m \rangle + \langle H_E \rangle(\mu) + \langle H_g \rangle(\mu) + \frac{1}{4} \langle H_a \rangle,$$

- $\langle T_{\mu\nu} \rangle$ expectation value of energy momentum tensor in hadron

- quark condensate $H_m = \sum_{u,d,s\dots} \int d^3x m \bar{\psi}\psi$

- quark energy $H_E = \sum_{u,d,s\dots} \int d^3x \bar{\psi}(\vec{D} \cdot \vec{\gamma})\psi$

- glue field energy $H_g = \int d^3x \frac{1}{2}(B^2 - E^2)$

- anomaly term

$$H_a = \sum_{u,d,s\dots} \int d^3x \gamma_m m \bar{\psi}\psi - \int d^3x \frac{\beta(g)}{g}(E^2 + B^2)$$

- $\langle H_m \rangle$, $\langle H_a \rangle$, $\langle H_E + H_g \rangle$ scale and scheme independent

- obtain from renormalized quark and gluon momentum fractions

$$\langle H_g \rangle = \frac{3}{4}M\langle x \rangle_g \quad \text{and} \quad \langle H_E \rangle = \frac{3}{4}M\langle x \rangle_q - \frac{3}{4}\langle H_m \rangle$$

- anomaly term from $\langle H_a \rangle = M - \langle H_m \rangle$

Proton mass decomposition (con't)

- determined mass M from two-point correlator
- used previous determination of $\langle H_m \rangle$ (2016)
- momentum fractions from

$$\langle x \rangle_{q,g} \equiv -\frac{\langle N | \frac{4}{3} \bar{T}_{44}^{q,g} | N \rangle}{M \langle N | N \rangle},$$

$$\bar{T}_{44}^q = \int d^3x \bar{\psi}(x) \frac{1}{2} (\gamma_4 \overleftrightarrow{D}_4 - \frac{1}{4} \sum_{i=0,1,2,3} \gamma_i \overleftrightarrow{D}_i) \psi(x),$$

$$\bar{T}_{44}^g = \int d^3x \frac{1}{2} (E(x)^2 - B(x)^2).$$

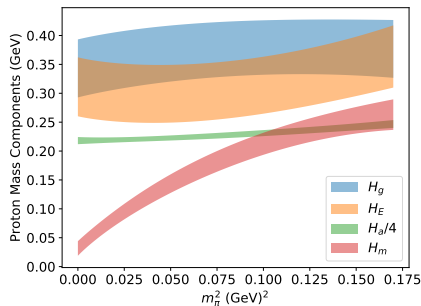
- renormalization

$$\langle x \rangle_{u,d,s}^R = Z_{QQ}^{\overline{\text{MS}}}(\mu) \langle x \rangle_{u,d,s} + \delta Z_{QQ}^{\overline{\text{MS}}}(\mu) \sum_{q=u,d,s} \langle x \rangle_q + Z_{QG}^{\overline{\text{MS}}}(\mu) \langle x \rangle_g$$

$$\langle x \rangle_g^R = Z_{GQ}^{\overline{\text{MS}}}(\mu) \sum_{q=u,d,s} \langle x \rangle_q + Z_{GG}^{\overline{\text{MS}}} \langle x \rangle_g,$$

Proton mass decomposition (con't)

- obtained results on 4 ensembles ($N_f = 2 + 1$ DWF action, overlap valence)
- disconnected insertions: cluster-decomposition error reduction, all time slices looped over
- extrapolate with global fit including finite volume, spacing corrections, chiral behavior



- quark energy 32(4)(4)%
- glue energy 36(5)(4)%
- quark condensate 9(2)(1)%
- trace anomaly 23(1)(1)%
- with $N_f = 2 + 1$

Nucleon spin decomposition

- spin decomposition of nucleon
[C.Alexandrou, M.Constantinou, K.Hadjjiyiannakou, K.Jansen, C.Kallidonis, G.Koutsou, A.V.Avilés-Casco, C.Wiese, PRL 119, 142002 (2017)]
- from Ji sum rule [Ji, PRL78, 610 (1997)]

$$J_N = \sum_{q=u,d,s,c,\dots} \left(\frac{1}{2} \Delta \Sigma_q + L_q \right) + J_g$$

- obtain from nucleon matrix elements ($Q=p'-p$, $P=\frac{1}{2}(p'+p)$)

$$\begin{aligned} \langle N(p, s') | \bar{q} \gamma_\mu \gamma_5 q | N(p, s) \rangle &= \bar{u}_N(p, s') \left[g_A^q \gamma^\mu \gamma_5 \right] u_N(p, s), \\ \langle N(p', s') | \bar{q} \gamma^{\{\mu} \overleftrightarrow{D}^{\nu\}} q | N(p, s) \rangle &= \bar{u}_N(p', s') \Lambda_{\mu\nu}^q(Q^2) u_N(p, s), \\ \Lambda_{q(g)}^{\mu\nu}(Q^2) &= A_{20}^{q(g)}(Q^2) \gamma^{\{\mu} P^{\nu\}} + B_{20}^{q(g)}(Q^2) \frac{\sigma^{\{\mu\alpha} q_\alpha P^{\nu\}}}{2m} \\ &\quad + C_{20}^{q(g)}(Q^2) \frac{1}{m} Q^{\{\mu} Q^{\nu\}}, \end{aligned}$$

Nucleon spin decomposition (con't)

- quark(gluon) total angular momentum and quark momentum fraction and spin from

$$\begin{aligned} J_{q(g)} &= \frac{1}{2}[A_{20}^{q(g)}(0) + B_{20}^{q(g)}(0)] \\ \langle x \rangle_q &= A_{20}^q(0), \quad \Delta\Sigma_q = g_A^q \end{aligned}$$

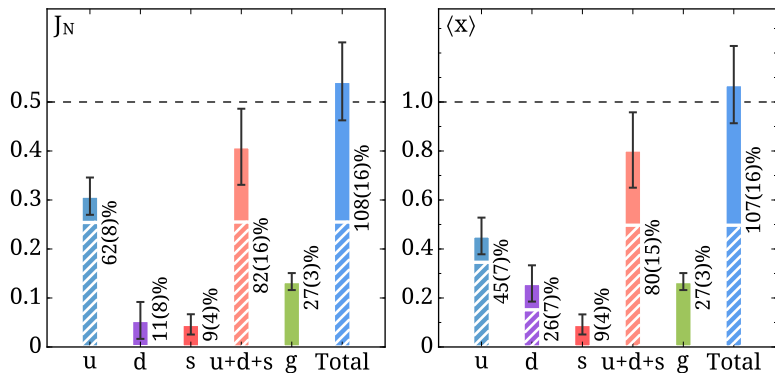
- gluon momentum fraction from $\mathcal{O}_{\mu\nu}^g = 2\text{Tr}[G_{\mu\sigma}G_{\nu\sigma}]$ with $\bar{\mathcal{O}}^g \equiv \mathcal{O}_{44}^g - \frac{1}{3}\mathcal{O}_{jj}^g$

$$\langle N(p, s') | \bar{\mathcal{O}}^g | N(p, s) \rangle = \left(-4E_N^2 - \frac{2}{3}p^2 \right) \langle x \rangle_g,$$

- one ensemble at physical point $48^3 \times 96$ twisted mass clover-improved $a = 0.0939(3)$ fm from nucleon mass
- u, d disconnected diagrams by exact deflation + one-end-trick
- s disconnected diagrams by truncated solver method
- renormalization factors determined nonperturbatively

Nucleon spin decomposition (con't)

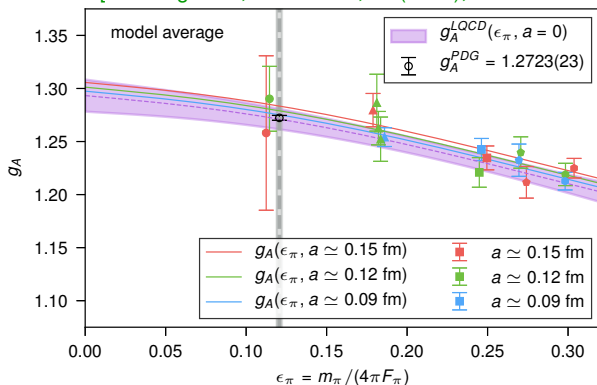
- nucleon spin (left) and momentum (right) decompositions
- striped segments \rightarrow valence; solid \rightarrow sea quark and gluon



Nucleon axial coupling

- recent percent level determination of g_A

[C.Chang et al., Nature 558, 91 (2018); arXiv:1805.12130]



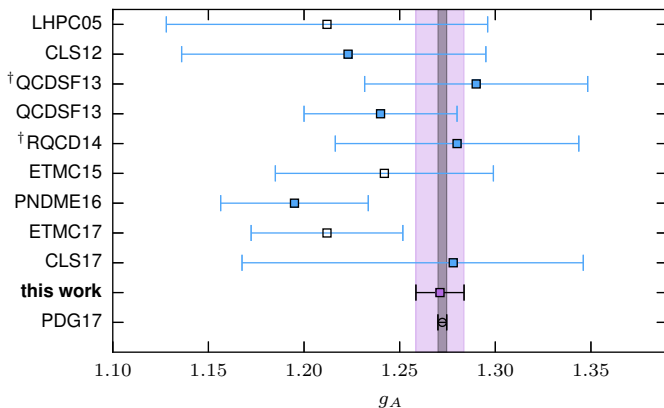
- use of Feynman-Hellman method

$$g_A = 1.2711(103)^s (39)^x (15)^a (19)^V (04)^I (55)^M$$

- errors: statistical, chiral, spacing, volume, isospin, model selection

Nucleon axial coupling (con't)

- comparison to other determinations

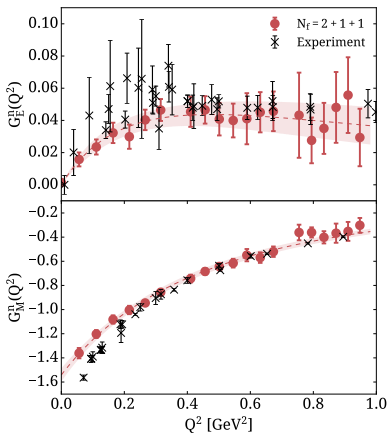
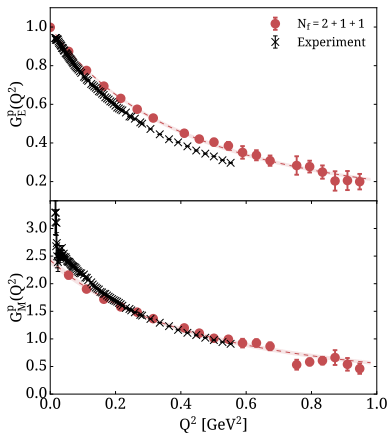


Proton/neutron electromagnetic form factors

- recent study of proton and neutron electromagnetic form factors
[C.Alexandrou, S.Bacchio, M.Constantinou, J.Finkenrath, K.Hadjiyiannakou, K.Jansen, G.Koutsou, A.V.Aviles Casco, arXiv:1812.10311]
- one ensemble $N_f = 2 + 1 + 1$ twisted mass with $m_\pi = 130$ MeV
- two ensembles $N_f = 2$ twisted mass with $m_\pi = 130$ MeV and two volumes $Lm_\pi \sim 3$ and $Lm_\pi \sim 4$
- unprecedented precision of disconnected diagram contributions
 - hierarchical probing
 - low mode deflation
 - large numbers of smeared point sources to reduce gauge noise
- disconnected diagrams have nonnegligible effects
- thorough investigation of excited-state contamination
- further study of finite-volume effects at low Q^2 needed

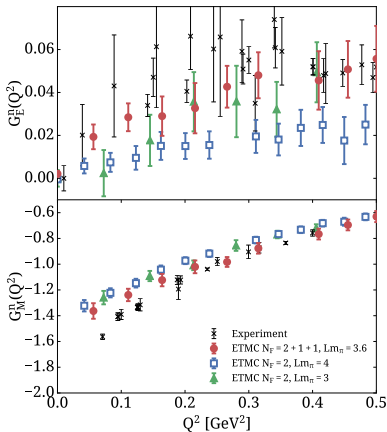
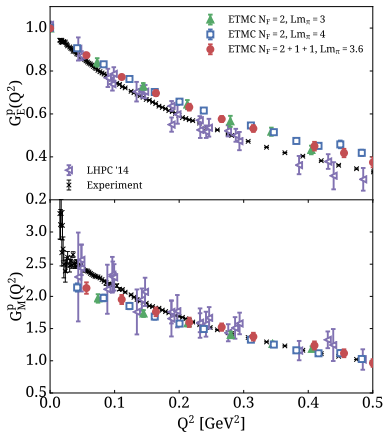
Proton/neutron electromagnetic form factors (con't)

- comparison of $N_f = 2 + 1 + 1$ results to experiment



Proton/neutron electromagnetic form factors (con't)

- comparing $N_f = 2 + 1 + 1$ and $N_f = 2$ (hollow symbols ignore disconnected)

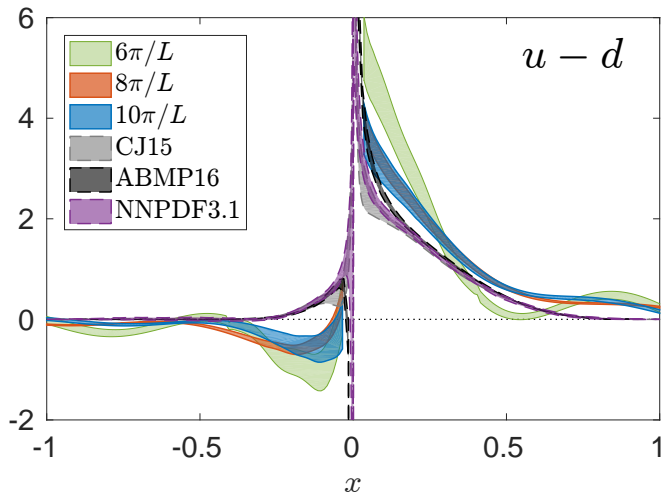


Light-cone parton distribution function

- first determination of unpolarized helicity parton distribution function at the physical point with nonperturbative renormalization and large momenta treated [C.Alexandrou, K.Cichy, M.Constantinou, K.Jansen, A.Scapellato, F.Steffens, PRL 121, 112001 (2018)]
- extracting PDFs from their moments impractical
- used method proposed by Ji [X.Ji, PRL110, 262002 (2013)] with subsequent refinements
 - compute spatial correlations between boosted nucleon states
 - Fourier transforms produce quasi-PDFs
 - take infinite-momentum limit via a refined matching procedure
 - target mass corrections
 - renormalization scheme for Wilson line operators
- one $48^3 \times 96$ twisted mass $N_f = 2$ ensemble $a = 0.0938(3)(2)$ fm and $m_\pi L = 2.98(1)$ at physical point

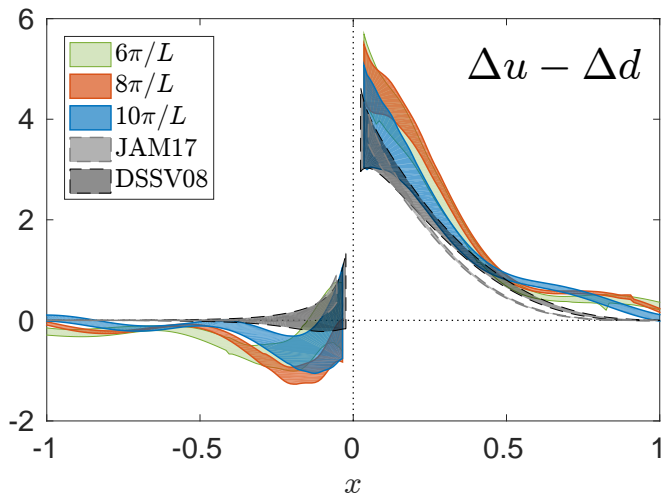
Light-cone parton distribution function (con't)

- unpolarized PDFs for three momenta compared to some phenomenological curves



Light-cone parton distribution function (con't)

- polarized PDFs for three momenta compared to some phenomenological curves



Conclusion

- stochastic LapH method works very well
 - allows evaluation of all needed quark-line diagrams
- large numbers of excited-state energy levels can be estimated
- scattering phase shifts can be computed
- infinite-volume resonance parameters from finite-volume energies below 2 particle thresholds
- time-like pion form factor computed
- scalar glueball determine in full QCD
- role of tetraquark operators
- string breaking revisited